



Contents lists available at ScienceDirect

# Spectrochimica Acta Part A: Molecular and Biomolecular Spectroscopy

journal homepage: [www.elsevier.com/locate/saa](http://www.elsevier.com/locate/saa)

## Novel mixed ligand complexes of bioactive Schiff base (*E*)-4-(phenyl (phenylimino) methyl) benzene-1,3-diol and 2-aminophenol/2-aminobenzoic acid: Synthesis, spectral characterization, antimicrobial and nuclease studies



P. Subbaraj<sup>a</sup>, A. Ramu<sup>b</sup>, N. Raman<sup>c,\*</sup>, J. Dharmaraja<sup>d</sup>

<sup>a</sup> Department of Chemistry, Devanga Arts College, Aruppukottai 626 101, Tamil Nadu, India

<sup>b</sup> Department of Inorganic Chemistry, School of Chemistry, Madurai Kamaraj University, Madurai 625 021, Tamil Nadu, India

<sup>c</sup> Research Department of Chemistry, VHNSN College, Virudhunagar 626 001, Tamil Nadu, India

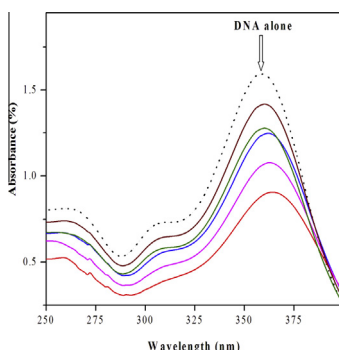
<sup>d</sup> Department of Chemistry, Sree Sowdambika College of Engineering, Aruppukottai 626 134, Tamil Nadu, India

### HIGHLIGHTS

- The synthesized metal complexes are good intercalators.
- The complexes are microcrystalline nature.
- Better antimicrobial active agents than the free ligand.
- Effective DNA cleavage activators.
- The Cu(II) complex is an excellent DNA binder.

### GRAPHICAL ABSTRACT

The (*E*)-4-(phenyl (phenylimino) methyl) benzene-1,3-diol derived Schiff base mixed ligand complexes act as good DNA binding and DNA cleaving agents. They are good antimicrobial activators.



### ARTICLE INFO

#### Article history:

Received 1 March 2013

Received in revised form 22 July 2013

Accepted 31 July 2013

Available online 8 August 2013

#### Keywords:

Benzophenone  
2-Aminophenol  
2-Aminobenzoic acid  
Metal complexes  
Antimicrobial activity  
DNA studies

### ABSTRACT

A novel bidentate Schiff base ligand has been synthesized using 2,4-dihydroxybenzophenone and aniline. Its mixed ligand complexes of **MAB** type [**M** = Mn(II), Co(II), Ni(II), Cu(II) and Zn(II); **HA** = Schiff base and **B** = 2-aminophenol/2-aminobenzoic acid] have been synthesized and characterized on the basis of spectral data UV-Vis, IR, <sup>1</sup>H NMR, FAB-Mass, EPR, SEM and magnetic studies. All the complexes were soluble in DMF and DMSO. Elemental analysis and molar conductance values indicate that the complexes are non-electrolytes. **HA** binds with M(II) ions through azomethine and deprotonated phenolic group and **B** binds through the primary amine group and deprotonated phenolic/carboxylic groups. Using FAB-Mass the cleavage pattern of the ligand (**HA**) has been established. All the complexes adopt octahedral geometry around the metal ions. It has been confirmed with the help of UV-Vis, IR, <sup>1</sup>H NMR and FAB-Mass spectral data. DNA binding activities of the complexes **1d** and **2d** are studied by UV-Vis spectroscopy and cleavage studies of Schiff base ligand and its complexes **1d** and **2d** have been by agarose gel electrophoresis method. *In vitro* biological activities of the free ligand (**HA**) and their metal complexes (**1a–1e** and **2a–2e**) were screened against few bacteria, *Escherichia coli*, *Staphylococcus saprophyticus*, *Staphylococcus aureus*, *Pseudomonas aeruginosa* and fungi *Aspergillus niger*, *Enterobacter species*, *Candida albicans* by well diffusion technique.

© 2013 Elsevier B.V. All rights reserved.

\* Corresponding author. Tel.: +91 92451 65958; fax: +91 4562 281338.

E-mail address: [drn\\_raman@yahoo.co.in](mailto:drn_raman@yahoo.co.in) (N. Raman).

## Introduction

Design and synthesis of new drugs of fewer side effects with unique properties is vital in medicinal inorganic chemistry [1]. At present, the bioactive novel Schiff base ligands containing N,O/S donor sites with transition metal complexes have considerable attention in the treatment of cancer cells in chemotherapeutic field [2–5]. Interaction of nucleic acid with metal complexes has been investigated to design the new types of pharmaceutical architecture, the mechanism involved in the site specific recognition of DNA and to determine the principles governing the recognition [6–9]. Mixed ligand complexes containing transition metals have considerable attention due to their effective DNA binding and cleavage activities under certain physiological conditions [10–14]. Hydroxybenzophenone and its derivatives exhibit good binding and cleavage behavior against DNA [15]. Their metal complexes show broad spectrum of pharmacological and clinical activities such as antibacterial, antifungal, antitumor and herbicidal [16–20]. Now-a-days greater attention has been given to the interaction of nucleic acids with Cu(II) and Ru(II) metal complexes [21] than the other metal complexes. These view encouraged us to design and synthesize novel bioactive mixed ligand complexes using NO type Schiff base ligand [(E)-4-(phenyl(phenylimino)methyl)benzene-1,3-diol; **HA**] with secondary ligand of 2-aminophenol/2-aminobenzoic acid (**B**).

In the sequel of our work [22], we have synthesized a novel bioactive bidentate NO type Schiff base ligand (**HA**) [(E)-4-(phenyl-phenylimino-methyl)-benzene-1,3-diol; obtained by the condensation of 2,4-dihydroxybenzophenone with aniline]. Moreover, we synthesized MAB type of mixed ligand complexes using this Schiff base ligand (**HA**) as primary ligand and 2-aminophenol/2-aminobenzoic acid (**B**) as co-ligand (s) with few transition bivalent M(II) ions [M = Mn, Co, Ni, Cu and Zn]. They are characterized by both physico-chemical and various spectral methods. DNA binding behavior of the metal complexes has been explored by electronic absorption spectral technique and cleavage are done by gel electrophoresis method under oxidative condition. Further, we have accounted for the biocidal activities against few pathogenic bacterial and fungal strains.

## Experimental

### Materials and methods

2,4-Dihydroxybenzophenone (extra pure) and aniline were purchased from Sigma Aldrich and S.D. Fine, respectively. 2-aminophenol, 2-aminobenzoic acid and metal chlorides were obtained from Merck products. In this study, all the chemicals have been used as such without any further purification. All the solvents were purified according to the literature. Calf Thymus (CT) DNA and pUC-19 DNA were obtained from Genei, Bangalore. Agrose (Molecular Biology grade), ethidium bromide (EB) were from Sigma (USA). Tris-(hydroxymethyl)aminomethane-HCl (Tris-HCl) buffer solution was prepared using deionized and sonicated triple distilled water using a quartz water distillation setup. Melting points of all the mixed ligand complexes were determined in open glass capillaries and taken as such. C, H and N analyses of the free Schiff base ligand and its mixed ligand complexes were performed in CHN analyzer Calrlo Erba 1108, Heraeus. Metal contents were analyzed by the standard procedure. Elico conductivity bridge (Model No. CM-180) was used to measure the molar conductance of the free Schiff base ligand (**HA**) and the metal complexes in DMSO ( $1 \times 10^{-3}$  M). Vibration spectra were recorded in KBr disc medium in the range 400–4000  $\text{cm}^{-1}$  in Perkin-Elmer 783 series spectrophotometer. Magnetic susceptibility measurement of the powdered samples

was carried out by the Gouy balance. Electronic spectra of free Schiff base ligand and the metal complexes were recorded in DMSO medium ( $1 \times 10^{-4}$  M) using Shimadzu UV-1601 spectrophotometer at ambient temperature.  $^1\text{H}$  NMR spectra of the ligand (**HA**) and its diamagnetic zinc complexes (**1e** and **2e**) in DMSO- $d_6$  medium were recorded on a Bruker Advance DRX 300 FT-NMR spectrometer using TMS as internal standard. Fast atomic bombardment mass spectra (FAB-MS) of the ligand (**HA**) and their metal complexes were recorded in VGZAB HS spectrometer using 3-nitrobenzoyl alcohol matrix. X-band EPR spectra of Cu(II) complexes were recorded in DMSO at room temperature (300 K) and liquid nitrogen conditions (77 K) on VARIAN E-112 EPR spectrometer using TCNE as internal standard. Thermogravimetric (TGA) analysis of the mixed ligand complexes was recorded on Perkin Elmer (TGS-2 model) thermal analyzer with heating rate of 10 K/min at  $\text{N}_2$  atmosphere (flow rate 20 mL/min). Scanning Electron Micrography (SEM) was used for morphological evaluation.

### Synthesis of Schiff base ligand (**HA**) and its mixed ligand complexes

#### Synthesis of Schiff base ligand [4-(phenyl-phenylimino-methyl)-benzene-1,3-diol; **HA**]

Hot ethanolic solution (20 mL) of 2,4-dihydroxybenzophenone (2.14 g, 10 mmol) was added drop wise into an ethanolic solution (20 mL) of aniline (0.93 g, 10 mmol). The resultant mixture was refluxed for 6 h under stirring (Scheme 1) (Supplementary data file). Then it was reduced to 1/3 of its original volume and kept aside at room temperature for evaporation. The yellow crystalline solid product separated was recrystallized from the same solvent. Yield: 85%.

#### Synthesis of complexes (**1a–1e**)

To 10 mL of ethanolic solution of Schiff base ligand (0.287 g, 1 mmol), 10 mL of ethanolic solution of metal(II) chloride (1 mmol) was added drop wise. The mixture was stirred continuously for 2 h. To this solution, 10 mL of hot ethanolic solution of 2-aminophenol (0.109 g, 1 mmol) was added and refluxed for 4–6 h. The resultant solution was reduced to one-third of its volume, filtered and evaporated to dryness. The obtained solid precipitate was washed with water and cold ethanol. It was dried *in vacuo*.

#### Synthesis of complexes (**2a–2e**)

To 10 mL of ethanolic solution of Schiff base ligand (0.287 g, 1 mmol) was added drop wise to the ethanolic solution (10 mL) of metal(II) chlorides (1 mmol) and stirred for 2 h. To this solution, 10 mL of hot ethanolic solution of 2-aminobenzoic acid (0.137 g, 1 mmol) was added and refluxed for 4–6 h. The resultant solution was reduced to one-third of its volume, filtered and evaporated to dryness. The solid product thus obtained was washed with water followed by cold ethanol and dried *in vacuo*.

### Antimicrobial studies

*In vitro* biological screening effects of the synthesized free Schiff base ligand and the mixed ligand complexes were done against the bacterial strains, *Escherichiacoli*, *Staphylococcussaphyphiticus*, *Staphylococcus aureus*, *Pseudomonas aeruginosa* and fungal strains, *Aspergillusniger*, *Enterobacterspecies*, *Candida albicans* by well diffusion method [23]. The same procedure [24] was followed for the determination of zone inhibition of the synthesized free ligand (**HA**) and the mixed ligand complexes against standard controls.

### Nuclease studies

The concentration of CT DNA was determined by UV absorbance at 260 nm ( $\epsilon = 6600 \text{ M}^{-1}\text{cm}^{-1}$ ). CT DNA free from protein

contamination was confirmed from its absorbance values at 260 nm, 280 nm and the ratio  $A_{260}/A_{280}$  was found to be 1.87 [25]. Stock solutions were kept at 4 °C and used after not more than four days. To prepare buffer and other solutions redistilled water free from CO<sub>2</sub> have been used.

#### Absorption studies

The electronic absorption spectra of mixed ligand complexes were recorded in the absence and presence of CT-DNA in DMSO medium. Absorption titrations were done by keeping the complex concentration (in 10<sup>-5</sup> M) as constant and varying the DNA concentration (0–50 μM). Binding experiments were done in DMSO solution [26–28] using Tris–HCl/NaCl buffer (5 mM Tris–HCl, 5 mM NaCl, pH = 7.2). Absorption spectra were recorded after successive addition of CT-DNA to the complex solution. The intrinsic binding constant ( $K_b$ ) was calculated according to the following equation:

$$\frac{[\text{DNA}]}{(\epsilon_a - \epsilon_f)} = \frac{[\text{DNA}]}{(\epsilon_b - \epsilon_f)} + \frac{1}{K_b(\epsilon_b - \epsilon_f)}$$

where  $\epsilon_f$ ,  $\epsilon_b$  and  $\epsilon_a$  are the molar extinction coefficients of the free complex in solution, complex in the completely bound form with CT-DNA and complex bound to DNA at a definite concentration respectively. In the plot of  $[\text{DNA}]/(\epsilon_a - \epsilon_f)$  versus  $[\text{DNA}]$ ,  $K_b$  was calculated.

#### Cleavage studies

*pUC-19* DNA at pH 7.5 in Tris–HCl buffered solution was used to perform the gel electrophoresis technique. Oxidative cleavage of DNA was examined keeping the concentration of the complexes 30 μM and 2 μL of *pUC-19* DNA was added and made up the volume to 16 μL using 5 mM Tris–HCl/5 mM NaCl buffer solution. The resulting solution was incubated at 37 °C for 2 h after the addition of DNA. 2 μL of 25% bromophenol blue was added to quench the reaction. The samples were electrophoresed for 2 h at 50 V in Tris–acetate–EDTA (TAE) buffer using 1% agarose gel containing 1.0 μg/mL ethidium bromide (EB) and photographed under UV light.

## Results and discussion

The bidentate NO type of Schiff base ligand (**HA**) and its mixed ligand complexes with 2-aminophenol/2-aminobenzoic acid (**B**) were synthesized and characterized by various spectral techniques. The synthesized mixed ligand complexes were found to be air stable, amorphous nature, moisture free and soluble only in DMF and DMSO.

#### Elemental analysis and conductivity measurements

The synthesized Schiff base ligand (**HA**) and the mixed ligand complexes of MAB type were investigated using various physico-chemical properties like melting point (m.p.), color, yield, elemental analysis and conductance values which are given in Table 1. The elemental analytical data of ligand (**HA**) and its MAB complexes agreed well with the calculated values, showing the 1:1:1 (M:A:B) stoichiometry ratio of the complexes (Fig. 1). The low molar conductance of the complexes indicates their non-electrolytic nature [29].

#### Vibrational spectral studies

Vibrational spectra of free Schiff base (**HA**) and 2-aminophenol (2-AP)/2-aminobenzoic acid (2-ABA) ligands (**B**) were compared to investigate the mode of binding present in the synthesized mixed ligand complexes. The ligand showed strong bands at 1245 and 1598 cm<sup>-1</sup> which are assigned to deprotonated phenolic-O and azomethine-N atoms and these bands were shifted to lower regions in the complexes which indicate that the ligand acts as bidentate manner in the metal chelates [30]. Free ligand (**B**) of 2-aminophenol showed a band at 3380 cm<sup>-1</sup> for ν(NH<sub>2</sub>) and 1265 cm<sup>-1</sup> for ν(OH) vibrations. Similarly, 2-aminobenzoic acid (**B**) showed a band at 3360 cm<sup>-1</sup> for ν(NH<sub>2</sub>) and 1498 cm<sup>-1</sup> for ν(COOH) vibrations. On complexation, the phenolic-O band was shifted to higher region (1275–1262 cm<sup>-1</sup>) in all the complexes and the azomethine-N band was shifted to the lower frequency region (1582–1560 cm<sup>-1</sup>). The ligands (**B**) bind with the M(II) ions in a bidentate manner through amine-N and deprotonated phenolic-O or carboxylate-O atoms, respectively. In **1a–1e** and **2a–2e** complexes, **HA** and **B** form stable 6, 5 and 6, 6 membered chelation

**Table 1**  
Elemental and physical data of ligand and its complexes.

Complex	Empirical formula	Formula weight	Color	m.p. (°C)	Yield (%)	Elemental analysis Found (Calc.)%				$\Lambda_M$ (Ω <sup>-1</sup> mol <sup>-1</sup> cm <sup>2</sup> )
						M	C	H	N	
<b>HA</b>	C <sub>19</sub> H <sub>17</sub> NO <sub>2</sub>	289	Yellow		85	–	78.79 (79.10)	4.64 (4.79)	11.34 (11.25)	–
<b>1a</b>	C <sub>25</sub> H <sub>24</sub> MnN <sub>2</sub> O <sub>5</sub>	487	Reddish brown	280	65	10.88 (11.10)	61.32 (61.51)	4.73 (4.80)	5.74 (5.62)	12.5
<b>1b</b>	C <sub>25</sub> H <sub>24</sub> CoN <sub>2</sub> O <sub>5</sub>	491	Pink	286	58	11.12 (11.25)	60.81 (61.10)	4.79 (4.92)	5.49 (5.58)	14.1
<b>1c</b>	C <sub>25</sub> H <sub>24</sub> NiN <sub>2</sub> O <sub>5</sub>	491	Pale green	>280	60	11.55 (11.72)	60.54 (60.85)	4.76 (4.85)	5.78 (5.65)	19.3
<b>1d</b>	C <sub>25</sub> H <sub>24</sub> CuN <sub>2</sub> O <sub>5</sub>	496	Brown	>280	55	12.52 (12.75)	60.18 (60.45)	4.65 (4.78)	5.51 (5.60)	16.8
<b>1e</b>	C <sub>25</sub> H <sub>24</sub> ZnN <sub>2</sub> O <sub>5</sub>	497	Pale yellow	>280	62	12.86 (13.12)	60.04 (60.31)	4.69 (4.76)	5.64 (5.53)	20.1
<b>2a</b>	C <sub>26</sub> H <sub>24</sub> MnN <sub>2</sub> O <sub>6</sub>	514	Brown	272	54	10.42 (10.66)	60.36 (60.57)	4.64 (4.75)	5.58 (5.44)	16.4
<b>2b</b>	C <sub>26</sub> H <sub>24</sub> CoN <sub>2</sub> O <sub>6</sub>	519	Violet	279	61	11.09 (11.35)	59.86 (60.12)	4.53 (4.65)	5.29 (5.40)	13.6
<b>2c</b>	C <sub>26</sub> H <sub>24</sub> NiN <sub>2</sub> O <sub>6</sub>	519	Green	284	69	11.16 (11.31)	59.93 (60.15)	4.52 (4.66)	5.52 (5.35)	18.2
<b>2d</b>	C <sub>26</sub> H <sub>24</sub> CuN <sub>2</sub> O <sub>6</sub>	524	Dark brown	>285	70	11.80 (12.12)	59.34 (59.58)	4.49 (4.61)	5.18 (5.31)	15.9
<b>2e</b>	C <sub>26</sub> H <sub>24</sub> ZnN <sub>2</sub> O <sub>6</sub>	525	Yellow	>285	63	12.21 (12.44)	59.07 (59.38)	4.44 (4.60)	5.05 (5.25)	21.8

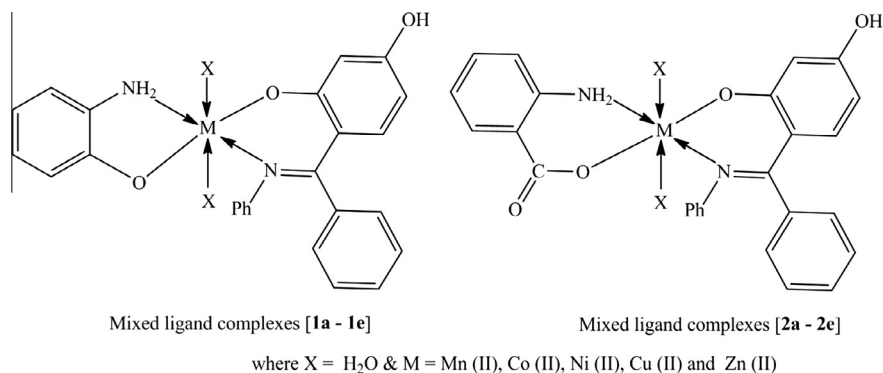


Fig. 1. Proposed structure of mixed ligand complexes.

Table 2  
Vibration spectral data for free ligand (**HA**) and mixed ligand complexes in KBr disk (cm<sup>-1</sup>).

Complex	$\nu(\text{H}_2\text{O})$	$\nu(\text{OH})_{\text{phen}}$	$\nu(\text{C}=\text{N})$	$\nu(\text{NH}_2)$	$\nu(\text{OH})$	$\nu(\text{COOH})$	$\nu(\text{M}-\text{O})$	$\nu(\text{M}-\text{N})$
2-AP <sup>a</sup>	–	–	–	3380,946	1265	–	–	–
2-ABA <sup>b</sup>	–	–	–	3360,924	–	1498	–	–
HA <sup>c</sup>	–	1245	1598	–	–	–	–	–
1a	3335,810,708	1266	1576	3365,925	3188,1281	–	421	551
1b	3320,822,714	1270	1582	3350,918	3192,1284	–	445	569
1c	3340,830,710	1262	1578	3361,922	3196,1277	–	465	573
1d	3320,840,716	1269	1580	3355,920	3185,1286	–	449	585
1e	3345,825,715	1274	1579	3359,916	3189,1295	–	440	571
2a	3330,838,720	1269	1570	3344,912	–	1466	432	559
2b	3355,825,709	1275	1574	3338,906	–	1472	451	564
2c	3340,844,712	1266	1580	3332,904	–	1469	460	570
2d	3335,838,714	1271	1576	3342,914	–	1460	449	563
2e	3320,850,710	1268	1579	3349,909	–	1468	464	575

<sup>a</sup> 2-AP = 2-aminophenol.

<sup>b</sup> 2-ABA = 2-aminobenzoic acid.

<sup>c</sup> HA = Schiff base ligand.

respectively. Further, the two new bands appeared in the far infrared region at 421–465 and 551–585 cm<sup>-1</sup> were assigned to  $\nu(\text{M}-\text{O})$  and  $\nu(\text{M}-\text{N})$  respectively [31]. The broad diffuse band at 3320–3355 cm<sup>-1</sup> and few bands appeared at 810–850 cm<sup>-1</sup> and 708–720 cm<sup>-1</sup> are attributed to the stretching, rocking and wagging mode of  $\nu(\text{OH})$  vibration of the coordinated water (OH<sub>2</sub>) molecules present in the complexes [31]. These are presented in Table 2.

#### FAB mass spectra

FAB mass spectrum (Fig. S1) (Supplementary data file) of the isolated Schiff base ligand (**HA**) showed the fragmentation pattern along with  $m/z$  value observed at 287 [ $M+1$ ] and the most intense peaks ( $m/z$ ) at 215, 185, 138 and 104, corresponding to the fragments of [C<sub>13</sub>H<sub>10</sub>NO<sub>2</sub>], [C<sub>13</sub>H<sub>11</sub>N], [C<sub>7</sub>H<sub>5</sub>NO<sub>2</sub>] and [C<sub>6</sub>H<sub>5</sub>O<sub>2</sub>]<sup>+</sup> respectively (Fig. S2) (Supplementary data file). This fragmentation pattern confirmed the proposed structure of the ligand (**HA**). The mass spectra of the complexes (**1c–1d** and **2c–2d**) exhibited  $m/z$  peaks at 493, 498, 521 and 524 with [ $M+2$ ] pattern respectively and which evidently support the composition of the mixed ligand complexes. Thus, the FAB spectral results confirm the stoichiometry composition presenting in free ligand (**HA**) and MAB complexes which reinforce the conclusion drawn from the elemental analysis data.

#### <sup>1</sup>H NMR spectra

Proton NMR spectrum of **HA** was compared with the diamagnetic mixed ligand Zn(II) complexes of **1e** and **2e** in DMSO-*d*<sub>6</sub>

medium using TMS (tetramethylsilane) as internal standard. The free ligand (**HA**) showed a group of multiplet signals at 6.4–7.6 due to phenyl moiety. The signals at 11.94 (s, 1H, OH) and 10.75 ppm (s, 1H, OH) are due to phenolic-OH group present in Schiff base ligand. Disappearance of peak at 10.75 ppm in the complexes (**1e** and **2e**) is due to the deprotonated phenolic-O group involved in the chelation. Downfield shifting of azomethine (–HC=N–) group in free ligand from 8.45 ppm to 8.27 and 8.22 ppm in the complexes of **1e** and **2e** respectively indicates that the azomethine group is involved in the complexation. New peaks appeared between 4.72 and 4.85 ppm in the complexes indicate the presence of coordinated water molecules.

#### Electronic spectra and magnetic moment values

Electronic spectra of **HA** and the mixed ligand complexes were recorded (10<sup>-3</sup> M, in DMSO solution) at room temperature. Absorption regions, band assignments, proposed geometry and the ligand field parameters are given in Table 3. **HA** showed three bands at 40,816, 34,364 and 29,411 cm<sup>-1</sup>, the first two bands are attributed to  $\pi \rightarrow \pi^*$  transition of benzene moieties and the other band is due to intra molecular charge transfer transition of  $n \rightarrow \pi^*$  respectively [29,30]. Mn(II) complexes (**1a** and **2a**) exhibited three weak absorption bands at 24,155–24,245, 20,284–20,452 and 13,805–13,650 cm<sup>-1</sup> regions which are assigned to <sup>6</sup>A<sub>1g</sub> → <sup>4</sup>T<sub>1g</sub>(<sup>4</sup>G) ( $\nu_3$ ), <sup>6</sup>A<sub>1g</sub> → <sup>4</sup>T<sub>2g</sub>(<sup>4</sup>G) ( $\nu_2$ ) and <sup>6</sup>A<sub>1g</sub> → <sup>4</sup>A<sub>1g</sub>, <sup>4</sup>E<sub>g</sub> (<sup>4</sup>G) ( $\nu_1$ ) transitions respectively [30]. The observed magnetic moment values of the above complexes (5.44–5.63 BM) are slightly lower than high spin complexes (6.0 BM) expected for five unpaired electron with an octahedral environment around Mn(II) ion

**Table 3**Electronic absorption spectral data (in DMSO) and magnetic susceptibility of the mixed ligand complexes (**1a–1e** and **2a–2e**) at 310 K.

Complex	$\lambda_{max}$ (cm <sup>-1</sup> )	Band assignments	Geometry	$\mu_{eff}$ (BM)	Ligand field parameter					
					Dq (cm <sup>-1</sup> )	B (cm <sup>-1</sup> )	$\beta$	$\beta$ (%)	LFSE (kJ mol <sup>-1</sup> )	$v_2/v_1$
<b>HA</b>	40,816	$\pi \rightarrow \pi^*$	-	-	-	-	-	-	-	-
	34,364	$n \rightarrow \pi^*$								
	29,411	INCT								
	24,155	${}^6A_{1g} \rightarrow {}^4T_{1g} ({}^4G)$								
<b>1a</b>	20,284	${}^6A_{1g} \rightarrow {}^4T_{2g} ({}^4G)$	Octahedral	5.44	-	-	-	-	-	-
	13,805	${}^6A_{1g} \rightarrow {}^4A_{1g} {}^4E_g ({}^4G)$								
	19,685	${}^4T_{1g} (F) \rightarrow {}^4T_{1g} (P)$								
<b>2b</b>	14,599	${}^4T_{1g} (F) \rightarrow {}^4A_{2g} (F)$	Octahedral	5.63	1520.3	783 (971 for free ion)	081	19.34	145.59	1.47
	9900	${}^4T_{1g} (F) \rightarrow {}^4T_{2g} (F)$								
	34,722	LMCT ( $n \rightarrow \pi^*$ )								
<b>1c</b>	25,794	${}^3A_{2g} (F) \rightarrow {}^3T_{1g} (P)$	Octahedral	3.18	1016	825 (1030 for free ion)	0.80	19.88	145.97	1.66
	16,891	${}^3A_{2g} (F) \rightarrow {}^3T_{1g} (F)$								
	10,162	${}^3A_{2g} (F) \rightarrow {}^3T_{2g} (F)$								
<b>1d</b>	14,528 (b)	${}^2E_g \rightarrow {}^2T_{2g}$	Octahedral	1.87	-	-	-	-	-	-
	26,254	LMCT ( $n \rightarrow \pi^*$ )	Octahedral	Dia.	-	-	-	-	-	Dia.
<b>2a</b>	24,245	${}^6A_{1g} \rightarrow {}^4T_{1g} ({}^4G)$	Octahedral	5.63	-	-	-	-	-	-
	20,452	${}^6A_{1g} \rightarrow {}^4T_{2g} ({}^4G)$								
<b>2b</b>	13,650	${}^6A_{1g} \rightarrow {}^4A_{1g} {}^4E_g ({}^4G)$	Octahedral	5.75	1089.6	701 (971 for free ion)	0.72	27.76	104.34	1.51
	19,157	${}^4T_{1g} (F) \rightarrow {}^4T_{1g} (P)$								
	14,771	${}^4T_{1g} (F) \rightarrow {}^4A_{2g} (F)$								
<b>2c</b>	9766	${}^4T_{1g} (F) \rightarrow {}^4T_{2g} (F)$	Octahedral	3.14	1002	828 (1030 for free ion)	0.80	19.62	143.93	1.66
	34,843	LMCT ( $n \rightarrow \pi^*$ )								
	25,840	${}^3A_{2g} (F) \rightarrow {}^3T_{1g} (P)$								
	16,639	${}^3A_{2g} (F) \rightarrow {}^3T_{1g} (F)$								
<b>2d</b>	10,020	${}^3A_{2g} (F) \rightarrow {}^3T_{2g} (F)$	Octahedral	1.84	-	-	-	-	-	-
	14,311 (b)	${}^2E_g \rightarrow {}^2T_{2g}$								
<b>2e</b>	26,458	LMCT ( $n \rightarrow \pi^*$ )	Octahedral	Dia.	-	-	-	-	-	Dia.

[32–33]. Complexes **1b** and **2b** showed three bands in the regions 9766–9900, 14,599–14,771 and 19,157–19,685 cm<sup>-1</sup>, which are assigned to  ${}^4T_{1g} (F) \rightarrow {}^4T_{2g} (F)$ ,  ${}^4T_{1g} (F) \rightarrow {}^4A_{2g} (F)$  and  ${}^4T_{1g} (F) \rightarrow {}^4T_{1g} (P)$  respectively. The  $\mu_{eff}$  values of Co(II) complexes **1b** and **2b** (5.63 and 5.75 BM) indicate the presence of four unpaired electrons in the high spin six-coordinated octahedral Co(II) complexes [33].

The complexes (**1c** and **2c**) showed four absorption bands at 10,020–10,162, 16,639–16,891, 25,840–25,974 and 34,843–34,722 cm<sup>-1</sup> which may be assigned to  ${}^3A_{2g} (F) \rightarrow {}^3T_{2g} (F)$ ,  ${}^3A_{2g} (F) \rightarrow {}^3T_{1g} (F)$ ,  ${}^3A_{2g} (F) \rightarrow {}^3T_{1g} (P)$  and LMCT transitions respectively with octahedral geometry with  ${}^3A_{2g}$  as ground state in D<sub>4h</sub> symmetry [32,33]. The water molecules occupied on z-axis of Cartesian coordinate made them hexa coordination around Ni(II) ion. Absence of any band below 10,000 cm<sup>-1</sup> ruled out the possibility of a tetrahedral. The observed magnetic moment of Ni(II) complexes were 3.14–3.18 BM which correspond to two unpaired electrons per Ni(II) ion for six-coordinated octahedral geometry [33]. From the absorption bands, the ligand field parameters such as B, B', Dq/B', 10 Dq and  $\beta$  for Co(II) and Ni(II) complexes were calculated from Tanabe Saugano diagrams. The observed Racah parameter (B) value is less than the free ion (971 cm<sup>-1</sup> for Co(II) ion and 1030 cm<sup>-1</sup> for Ni(II) ion;  $\beta$  (0.72–0.81) and  $\beta$  (%) (19.34–27.76) values also support the covalent character of Co(II) and Ni(II) complexes with distorted octahedral geometry [34,35]. Complexes of **1d** and **2d** exhibited only one broad band centered at 14,528 and 14,311 cm<sup>-1</sup> which may be assigned to the  ${}^2E_g \rightarrow {}^2T_{2g}$  transition in an octahedral geometry respectively [33]. The observed  $\mu_{eff}$  values (1.87 and 1.84 BM) for complexes **1d** and **2d** indicate that the unpaired electron lies predominantly in  $d_{x^2-y^2}$  ground state with octahedral structure [31]. Diamagnetic nature of Zn(II) ion did not show any d–d transition in the visible region. However, the complexes (**1e** and **2e**) showed only one broad band at 26,254 and 26,458 cm<sup>-1</sup> due to L → M charge transfer in a distorted octahedral environment with  $sp^3d^2$  hybridization [33].

#### EPR spectra

The EPR spectra of the Cu(II) complexes (**1d** and **2d**) were recorded at room temperature and liquid nitrogen temperature (77 K). The g-tensor values were computed from the spectrum using tetracyanoethylene (TCNE) free radical as 'g' marker. From the observed spectrum, Cu(II) complexes (**1d** and **2d**) follow the g-tensor values as  $g_{||}$  (2.27 and 2.29) >  $g_{\perp}$  (2.01 and 2.03) >  $g_e$  (2.0027) which indicate that the unpaired electron is localized in  $d_{x^2-y^2}$  orbital of the Cu(II) ion with 3d<sup>9</sup> configuration [36] with considerable covalent nature [37] present in Cu–L. The observed  $g_{avg}$  value of these complexes is equal to 2.06–2.10 and deviated from  $g_e$  (2.0027) value due to the covalence property. The  $g_{||}$  value was well agreed with the other reported N<sub>2</sub>O<sub>2</sub> type complexes [37]. These values also give evidence for the elemental and vibrational studies of metal chelating environment. Absence of any half field signal at 1600 G corresponding to  $\Delta M_s = \pm 2$  transitions, ruling out any magnetic exchange i.e., Cu–Cu interactions in the complexes. The bonding parameters of  $\alpha^2$  and  $\beta^2$  values were calculated using Kivelson and Neimann formula and the observed values reflect higher covalence of the L–Cu bonding present in the mixed ligand complexes. Hyperfine structure observed corresponds to N<sub>2</sub>O<sub>2</sub> coordination mode in distorted octahedral environment present in Cu(II) complexes. Hathaway [38] pointed out that for the pure  $\pi$ -bonding,  $K_{||} > K_{\perp} \approx 0.77$  and for in-plane  $\pi$ -bonding  $K_{||} < K_{\perp}$ , while for out-of-plane  $\pi$ -bonding  $K_{||} > K_{\perp}$  the following simplified expressions were used to calculate  $K_{||}$  and  $K_{\perp}$ :

$$K_{||} = \left( \frac{g_{||} - 2.0023}{8\lambda_0} \right) \times \text{d-d transition}$$

$$K_{\perp} = \left( \frac{g_{\perp} - 2.0023}{2\lambda_0} \right) \times \text{d-d transition}$$

The observed  $K_{||} > K_{\perp}$  relation indicates the absence of significant in-plane  $\pi$ -bonding.

### Thermogravimetric analysis

TGA of mixed ligand complexes are used to (i) get information about the thermal stability, (ii) to decide whether the water molecules (if present) are inside or outside the coordination sphere and (iii) thermal decomposition of chelates [39]. In this present study, heating rates were  $10\text{ }^{\circ}\text{C min}^{-1}$  under nitrogen atmosphere. The Cu(II) complexes (**1d** and **2d**) were fairly stable at room temperature and by increasing the temperature up to  $200\text{ }^{\circ}\text{C}$ , there was a gradual weight loss up to 5–6% indicating the coordinated water molecules are present in the complexes. Above  $200\text{ }^{\circ}\text{C}$ , there was a sudden weight loss up to  $400\text{ }^{\circ}\text{C}$  which indicates the evaporation of organic ligand moiety. The decomposition of ligand molecules continued and leading to formation of air stable metal oxide as the end product at about  $780\text{ }^{\circ}\text{C}$  (Fig. S3) (Supplementary data file).

### SEM morphology analysis

The particle size and the surface structure of the mixed ligand complexes have been shown from the scanning electron micrograph (SEM) pictograph. Fig. S4 (Supplementary data file) illustrates the SEM photographs of the mixed ligand Ni(II) complexes (**1c** and **2c**). From the pictographs, the complexes have homogeneous matrix with even interface having ideal shape of uniform phase material. A bundle of irregularly broken straw like shape was observed for the complex (**1c**) with the particle size of  $\sim 9\text{ }\mu\text{m}$ . Particle size of the complex (**2c**) was obtained as  $10\text{ }\mu\text{m}$  with broken stemless mushroom pieces like shape. This leads to believe that we are dealing with homogeneous phase material.

### DNA binding studies

DNA binding interaction of mixed ligand complexes (**1d** and **2d**) were carried out by using electronic absorption techniques at  $37\text{ }^{\circ}\text{C}$ . Absorption spectra of synthesized Cu(II) complex (**1d**) in the absence and presence of DNA are shown in Fig. 2. With [DNA], the absorption intensity of the complexes decreased (hypochromic effect) [40] and the  $\lambda_{\text{max}}$  values were shifted to red region (bathochromic shift). The interaction of metal complexes with DNA leads to both hypochromic and bathochromic effects which indicate the intercalative binding mode, due to strong intercalation between the metal complexes and the base pairs of DNA. In this binding, there was a strong stacking interaction between the planer aromatic chromophores of the ligand with DNA base pairs. In the UV region, Cu(II) complexes (**1d** and **2d**) exhibited three bands at ca. 265–268, 310–315 and 360–368 nm under the same experimental conditions. The intrinsic binding constant values for Cu(II) complexes (**1d** and **2d**) were  $4.96 \times 10^5\text{ M}^{-1}$  and  $5.24 \times 10^5\text{ M}^{-1}$  respectively. From the intrinsic binding constant ( $K_b$ ), the free energy change values for the Cu(II) complexes (**1d** and **2d**) were calculated ( $-29.44$  and  $-31.10\text{ kJ mol}^{-1}$  respectively) and these results indicate that the mixed ligand complexes can interact with DNA in a spontaneous manner.

### Biological activity

*In vitro* microbial activities of free Schiff base ligand (**HA**) and MAB mixed ligand complexes (**1a–1e** and **2a–2e**) were tested against few pathogenic bacterial and fungal strains by well diffusion method using agar as nutrient at different concentrations (25, 50 and  $75\text{ }\mu\text{g}$ ). Commercially available standard drugs Ampicillin and Nystatin were used as antibacterial and antifungal controls respectively and the zone inhibition measurements against the controls are listed in Table 3. From Table 3, it is observed that all the complexes showed a remarkable biological activity at higher concentration ( $75\text{ }\mu\text{g}$ ) against microorganisms

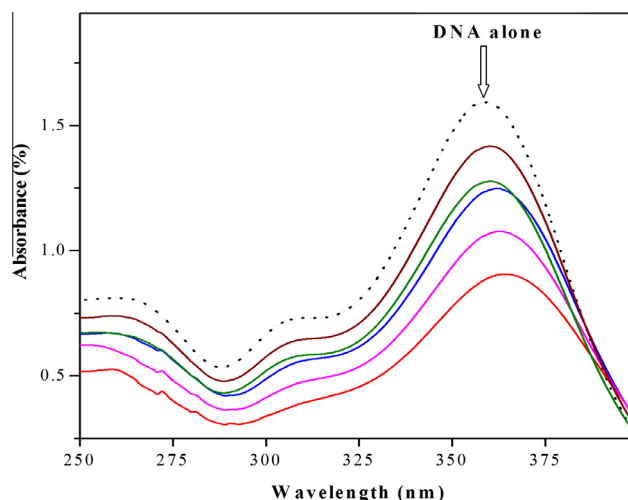


Fig. 2. Electronic absorption spectrum of complex (**1d**) in the absence (----) and presence (—) of increasing amount of CT DNA.

and this higher zone of inhibition can be explained on the basis of Overtone's concept and Tweedy's chelation theory [41–42]. All the mixed ligand complexes showed more considerable antibacterial than antifungal activities. A representative graph for the biological activity of Schiff base ligand (**HA**) and the MAB complexes is shown Fig. S5 (Supplementary data file). Biological activities of the metal complexes were found to be increased as the stability of the mixed ligand complexes increased and the activity of free Schiff base ligand (**HA**) and the MAB complexes followed the order which is given below:

**Control** > (**2d**) > (**2c**) > (**2b**) > (**2e**) > (**2a**) > **HA** and

**Control** > (**1d**) > (**1c**) > (**1b**)  $\approx$  (**1e**) > (**1a**) > **HA** complexes

### Oxidative cleavage

The oxidative cleavage activities of free Schiff base ligand (**HA**) and its Cu(II) complexes have been studied by gel electrophoresis and a representative pictograph is shown in Fig. S6 (Supplementary data file). The results showed that the supercoiled pUC19 DNA in buffer medium (pH = 7.2; Tris-HCl/NaCl) was converted into open circular form due to the formation of metal chelation. During the cleavage process, the smallest fragments moved quickly towards anode than the larger fragments. Bromophenol blue was used as a photosensitizer that can be activated on irradiation by UV. The completion of gel electrophoresis experiment clearly indicated that the intensity of the treated DNA samples has diminished due to the cleavage of DNA. The complex **1d** cleaved the DNA moderately than the complex **2d** and the Schiff base ligand. These results indicated that the metal ions played an important role in the cleavage of DNA.

### Conclusion

In this paper, a novel bidentate Schiff base ligand (**HA**) was synthesized using 2,4-dihydroxybenzophenone and aniline. Complexes of **MAB** type (**M** = Mn(II), Co(II), Ni(II), Cu(II) and Zn(II); **HA** = Schiff base; **B** = 2-aminophenol/2-aminobenzoic acid) were also synthesized and characterized by the spectral and analytical techniques. The UV-Vis, IR,  $^1\text{H}$  NMR, EPR and FAB-Mass data showed that all the complexes adopt octahedral geometry. XRD and SEM analyses indicated that the complexes are microcrystalline nature. From

DNA binding experiments it was concluded that the complexes are moderate intercalators. DNA cleavage indicated that the Cu(II) complex (**1d**) is a better cleaver than the Schiff base and **2d**. The antimicrobial data indicated that the complexes are having greater activity than the free Schiff base ligand.

### Acknowledgements

The authors communicate their sincere thanks to the Managing Board, Principal and Head of the Department of Devanga Arts College, Aruppukottai and VHNSN College, Virudhunagar for their moral support. They express their gratitude to SAIF, IIT-Madras, IIT Bombay and Punjab University for recording NMR, EPR and FAB-Mass spectra respectively and STIC, Cochin for TGA/DTA & SEM studies.

### Appendix A. Supplementary material

Supplementary data associated with this article can be found, in the online version, at <http://dx.doi.org/10.1016/j.saa.2013.07.096>.

### References

- [1] H.H. Xu, X. Tao, Y.Q. Li, Y.Z. Shen, Y.H. Wei, *Polyhedron* 33 (1) (2012) 347–352.
- [2] N. Raman, R. Jeyamurugan, R. Senthilkumar, B. Rajkapoor, S.G. Franzblau, *Eur. J. Med. Chem.* 45 (11) (2010) 5438–5451.
- [3] M.H. Habibi, E. Shojaee, M. Ranjbar, H.R. Memarian, A. Kanayama, T. Suzuki, *Spectrochim. Acta* 105A (2013) 563–568.
- [4] M.H. Habibi, E. Askari, *Synth. React. Inorg. Met.-Org. Nano-Met. Chem.* 43 (4) (2013) 400–405.
- [5] M.H. Habibi, E. Askari, *Synth. React. Inorg. Met.-Org. Nano-Met. Chem.* 43 (4) (2013) 406–411.
- [6] R.S. Kumar, S. Arunachalam, V.S. Periasamy, C.P. Preethy, A. Riyasdeen, M.A. Akbarsha, *Eur. J. Med. Chem.* 43 (10) (2008) 2082–2091.
- [7] M. Yodoshi, M. Odoko, N. Okabe, *Chem. Pharm. Bull.* 55 (6) (2007) 853–860.
- [8] K. Jiao, Q.X. Wang, W. Sun, F.F. Jian, *J. Inorg. Biochem.* 99 (6) (2005) 1369–1375.
- [9] H. Yin, H. Liu, M. Hong, *J. Organomet. Chem.* 713 (2012) 11–19.
- [10] L. Jia, J. Shi, Z. Sun, F. Li, Y. Wang, W. Wu, Q. Wang, *Inorg. Chim. Acta* 391 (2012) 121–129.
- [11] A.K. Patra, S. Roy, A.R. Chakravarty, *Inorg. Chim. Acta* 362 (5) (2009) 1591–1599.
- [12] H.T. Chifotides, K.M. Koshlap, L.M. Perez, K.R. Dunbar, *J. Am. Chem. Soc.* 125 (35) (2003) 10714–10724.
- [13] H.T. Chifotides, K.M. Koshlap, L.M. Perez, K.R. Dunbar, *J. Am. Chem. Soc.* 125 (35) (2003) 10703–10713.
- [14] C.A. Mitsopoulou, C. Dagas, *Bioinorg. Chem. Appl.* (2010) 1–10.
- [15] M.S.S. Babu, K.H. Reddy, P.G. Krishna, *Polyhedron* 26 (3) (2007) 572–580.
- [16] S. Mohan, J. Saravanan, *Asian J. Chem.* 15 (1) (2003) 67–70.
- [17] Y.S.R. Krishnaiah, M. Lakashmi, V. Satyanarayana, P. Bhaskhar, *Asian J. Chem.* 14 (2002) 1246–1250.
- [18] E.M. Hodnett, W.J. Dunn, *J. Med. Chem.* 13 (4) (1970) 768–770.
- [19] Z.M. Nofal, M.I. El-Zahar, S.S.A. El-Karim, *Molecules* 5 (2) (2000) 99–113.
- [20] S. Samadhiya, A. Halve, *Orient J. Chem.* 17 (1) (2001) 119–122.
- [21] G. Sathyaraj, T. Weyhermuller, B.U. Nair, *Eur. J. Inorg. Chem.* 45 (2010) 284–291.
- [22] N. Raman, R. Jeyamurugan, A. Sakhthivel, L. Mitu, *Spectrochim. Acta* 75A (2010) 88–97.
- [23] N. Raman, S. Sobha, *J. Serb. Chem. Soc.* 75 (2010) 1–16.
- [24] N. Raman, L. Mitu, A. Sakhthivel, M.S.S. Pandi, *J. Iran Chem. Soc.* 6 (4) (2009) 738–748.
- [25] N. Raman, S. Sudharsan, *Appl. Surf. Sci.* 257 (24) (2011) 10659–10666.
- [26] A. Hussain, S. Saha, R. Majumdar, R.R. Dighe, A.R. Chakravarty, *Ind. J. Chem.* 50A (2011) 519–530.
- [27] D. Crespy, K. Landfester, U.S. Schubert, A. Schiller, *Chem. Commun. (Camb)* 46 (36) (2010) 6651–6662.
- [28] N.J. Farrer, L. Salassa, P.J. Sadler, *Dalton Trans.* (2009) 10690–10701.
- [29] W.J. Geary, *Coord. Chem. Rev.* 7 (1971) 81–122.
- [30] K. Nakamoto, *Infrared and Raman Spectra of Inorganic and Coordination Compounds*, Wiley, New York, 1986.
- [31] L.J. Bellamy, *Infrared Spectra of Complex Molecules*, second ed., Mathuen, London, 1958.
- [32] T.M. Dunn, *The Visible and Ultraviolet Spectra of Complex Compounds in Modern Coordination Chemistry*, Wiley Interscience, New York, 1960.
- [33] A.B.P. Lever, *Electronic Spectra of d<sup>n</sup> Ions in Inorganic Electronic Spectroscopy*, second ed., Elsevier, Amsterdam, The Netherlands, 1984.
- [34] C.J. Ballhausen, *Introduction to Ligand Field Theory*, McGraw-Hill, New York, 1962.
- [35] E. Konig, *The Nephelauxetic Effect, in Structure and Bonding*, Springer Verlag, Berlin, New York, 1971.
- [36] R.L. Dutta, A. Syamal, *Electron spin resonance responses, in: Elements of Magnetochemistry*, second ed., East-West Press, New Delhi, 1992, pp. 206–250.
- [37] D. Kivelson, R. Neiman, *J. Chem. Phys.* 35 (1) (1961) 149–155.
- [38] R.J. Dudley, B.J. Hathaway, *J. Chem. Soc. A* (1970) 2794–2799.
- [39] A.M. Khedr, H.M. Marwani, *Int. J. Electrochem. Sci.* 7 (2012) 10074–10093.
- [40] S. Zhang, J. Zhou, *J. Coord. Chem.* 61 (15) (2008) 2488–2498.
- [41] Y. Anjaneyula, R.P. Rao, *Synth. React. Inorg. Met.-Org. Chem.* 16 (2) (1986) 257–272.
- [42] B.G. Tweedy, *Phytopathology* 55 (1964) 910–914.